Contents lists available at ScienceDirect

Sensors & Actuators: B. Chemical

journal homepage: www.elsevier.com

Cascade-Amplified Microfluidic Particle Accumulation Enabling Quantification of Lead Ions through Visual Inspection

Minghui Wu [1], Gaobo Wang [1], Lok Ting Chu , Hanjin Huang , Ting-Hsuan Chen *

Department of Biomedical Engineering, City University of Hong Kong, Hong Kong Special Administrative Region

ARTICLE INFO

Keywords:
Leads
Visual detection
DNAzyme
Catalytic hairpin assembly
Microparticles
Microfluidics

ABSTRACT

Exposure to lead in drinking water elevates blood lead levels and causes permanent impairment to human body. To provide a preventive measure for lead intoxication, here we report a sensitive visual quantification of lead in drinking water and whole blood. GR-5 DNAzyme can be cleaved by Pb^{2+}, releasing an oligonucleotide T that triggers catalytic assembly of hairpin complex H1H2 connecting magnetic microparticles (MMPs) and polystyrene microparticles (PMPs). After loading the particle solution into a capillary-driven microfluidic device, MMPs-H1H2-PMPs are first attracted and removed by a magnetic separator, and the remaining free PMPs continue flowing along the microchannel until accumulating at a particle dam. As such, more lead ions cause shorter PMP accumulation quantifiable by the naked eye. The method achieved a limit of detection (LOD) of 246 pM, and is extremely selective (> 40,000 folds to other metal ions), and highly tolerant to acidity/basicity (6 – 8.5) and water hardness (55 – 318.3 mg/L). More importantly, high recovery rate (> 78%) in tap water and LOD of 2.57 nM for lead level in whole blood were achieved, demonstrating a visual quantification method for screening water safety and lead intoxication with user-friendly interface.

1. Introduction

Lead ion is one of the most poisonous heavy metal ions commonly present in gasoline, batteries and pigments industries [1]. Due to its non-biodegradability, there are approximately 300 million tons of mined lead circulating in soil and groundwater, resulting in serious environmental pollution [1]. A very small amount of lead ions can cause many diseases in human body, such as neurological diseases, cardiovascular diseases, reproductive system diseases, developmental disorders, and increase the risk of permanent neurological damage and hypertension to children [2]. Therefore, there are urgent needs for monitoring the trace amounts of lead in drinking water for environment and food safety, or in blood for diagnosis of lead intoxication.

BLL (blood lead level) of concern is 5 μg/dL (241.3 nM) for children according to CDC Response to Advisory Committee on Childhood Lead Poisoning Prevention Recommendations, while the Environmental Protection Agency has defined 15 ppb (72.4 nM) as the action level for lead in tap water [3,4]. To monitor it, there are analytical techniques including atomic absorption spectrometry (AAS) [5], atomic fluorescence spectrometry (AFS) [6], inductively coupled plasma mass spectrometry (ICP-MS) [7], and capillary electrophoresis [8,9]. However, because costly instruments or complicated procedures are required, those methods are inconvenient, time-consuming and not suitable for end-users [10].

Recently, various chemo- and bio- sensors for Pb^{2+} detection have been employed using recognition materials, including proteins [11], peptides [12], nucleic acids [13] and small ligands [14]. Among them, DNAzyme has been extensively studied and attracted wide interest due to their numerous advantages of high stability, catalytic activity, low relative molecular weight, and simple synthesis and modification [15,16]. Pb^{2+}-specific DNAzyme GR-5 is usually utilized as the core of sensors to output signals such as fluorescence [17–24], electrochemistry [25–28], chemiluminescence [29–31] and colorimetry [32–37]. However, for those conventional signals, standard equipment such as spectrometer or ammeter is needed, which makes the analysis bulky and expensive. To make it more suitable for on-site and fast measurement through untrained end-users, miniaturized detection with simple and visible readout is more desired. There are attempts based on the appearance of a visible bar on lateral flow dipstick [38] and accumulation of nanoparticles in the microchannels [39]. In particular, quantitative measurements of lead were also allowed by the movement of

* Corresponding author.
Email address: thchen@cityu.edu.hk (T-H Chen)
[1] These authors contributed equally to this work.

https://doi.org/10.1016/j.snb.2020.128727
Received 14 May 2020; Received in revised form 1 August 2020; Accepted 7 August 2020
Available online xxx
0925-4005/

Table 1
Comparison of methods with visual readouts

Detection Concept	LOD	Sample-to-Result Time	Sample Matrix	Equipment/Instrumentation	Ref.
Dipstick test	0.5 μM	30 min	Pb^{2+} extracted from paints	No	[38]
Microfluidic chip	10 μM	15 min	Water	Microscope / Magnifier	[39]
Volumetric bar-chart chip	1.0 nM	40 min	DI water	No	[40]
Microfluidic chip	2.12 nM	65 min	Tap water	No	[41]
Microfluidic chip	246 pM	95 min (Tap water); 125 min (Whole blood / Plasma)	Tap water / Whole blood / Plasma	No	This work

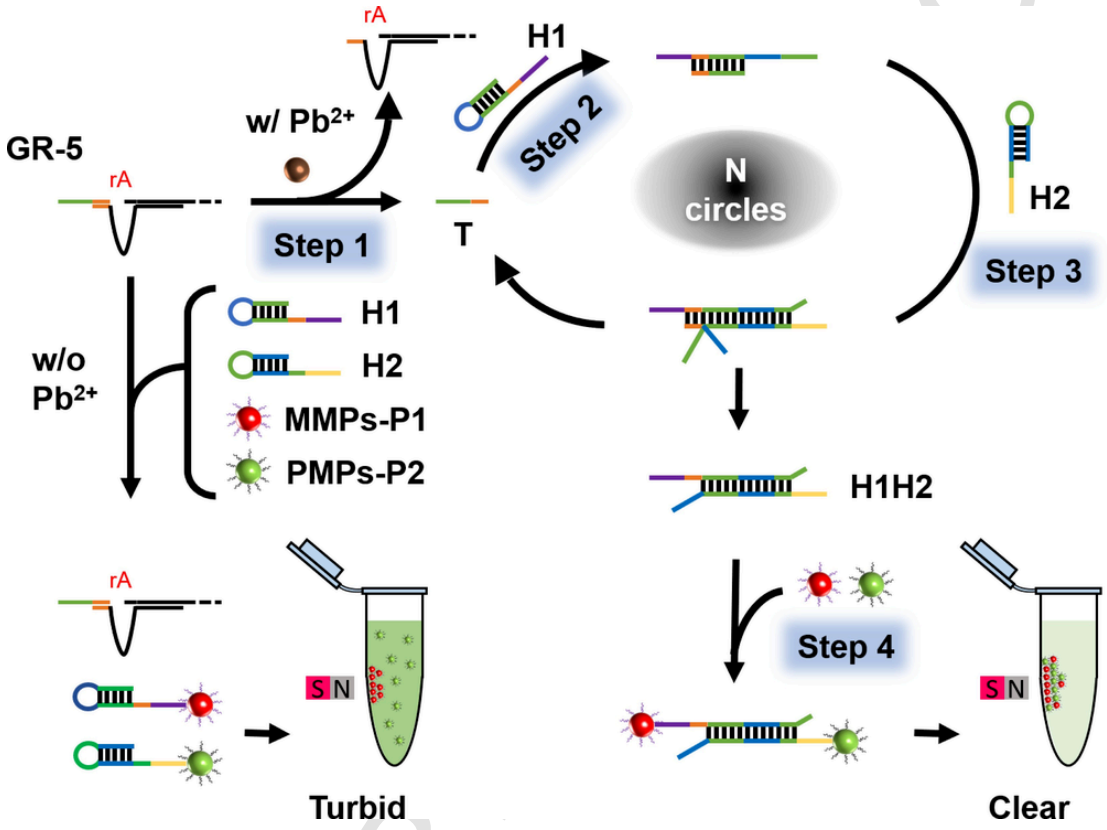

Fig. 1. Working principle of CHA triggered by the released T after GR-5 cleavage. First, GR-5 is cleaved by lead ions to release the oligonucleotide Target (T) (Step 1). With addition of H1 and H2, the T hybridizes with H1 and opens its hairpin structure (Step 2), which can subsequently open the H2 and then displace and release the T for the next cycle (Step 3). After repeating, it produces massive amount of assembled H1 and H2. H1-H2 complexes would hybridize with the biotinylated oligonucleotides P1 and P2 on streptavidin-coated MMPs and PMPs, respectively, leading to the formation of MMPs-H1H2-PMPs (Step 4). Finally, MMPs-P1 and MMPs-H1H2-PMPs would be attracted to the tube side wall resulting in clear solution. Otherwise, when there is no Pb^{2+} added, MMPs could not connectto PMPs, leaving the solution turbid.

an ink bar [40] or microparticle accumulation in microfluidic chip [41]. However, for visual detections, the LOD is mostly at nM/μM level, and detection in unprocessed, raw matrix such as blood is hardly achieved (Table 1).

In this work, a visual, quantitative, and sensitive method for lead ion detection is provided using cascade-amplified microfluidic particle accumulation. When lead ion is present, Pb^{2+}-specific GR-5 is cleaved to release a strand of oligonucleotide Target (T). Of note, oligonucleotides can be used for signal amplification such as hybridization chain reaction [42], catalytic hairpin assembly (CHA) [43], rolling circle amplification [44] and toehold-mediated strand displacement [45]. Because CHA is enzyme-free, free-energy-driven, convenient, and programmable in isothermal reactions [46–48], the released T is used to trigger CHA with hairpins H1 and H2 to amplify the production of T (Fig. 1). In follows, the mass-produced hairpin assembly H1H2 connects MMPs and PMPs, leading to the formation of MMPs-H1H2-PMPs. Next, a microfluidic system is applied. Microfluidics has become an enabling technology for point-of-care and personalized diagnostics because of low reagent consumption, high throughput and rapid analysis [49–54]. To visually quantify the particle connection, the particle solution is loaded onto a microfluidic device. Driven by capillary flow, MMPs-H1H2-PMPs are first removed by a magnetic separator, while free PMPs can continue flowing and eventually accumulate at a particle dam, forming a visual bar with a visible length inversely proportional to the amount of lead ions. Comparing to our previous method where MMPs and PMPs are connected by the GR-5 but separated after lead-mediated cleavage [41], here the T releaseded from GR-5 cleavage is used to trigger the CHA amplification. Thus, low concentration of lead can bring mass-produced hairpin assembly H1H2 to connect MMPs and PMPs, allowing great improvement of detection sensitivity. With validated particle connection based on Pb^{2+}-triggered CHA, the LOD of lead detection, selectivity, and tolerance to solution acidity/basicity and water hardness were investigated. Furthermore, tap water and whole blood were applied to demonstrate the visual and sensitive Pb^{2+} detection for monitoring water safety and lead intoxication.

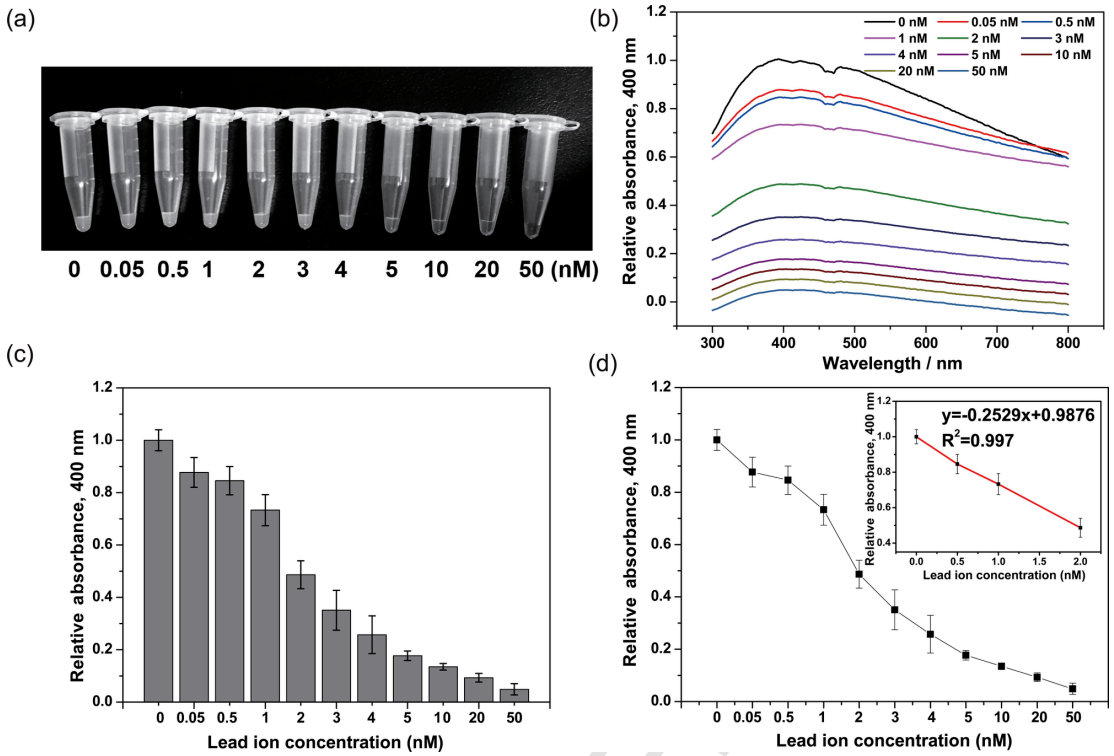

Fig. 2. Magnetophoresis assay for detection of lead ions. (a) Optical image of supernatant with suspending PMPs resulted from different concentrations of Pb^{2+} (0-50 nM). (b) Relative UV-Vis spectral absorbance corresponding to (a). (c) Relative spectral absorbance at 400 nm. (d) Linear regression of the relative spectral absorbance at 400 nm of varying concentrations of Pb^{2+} (mean ± max deviation, n = 3).

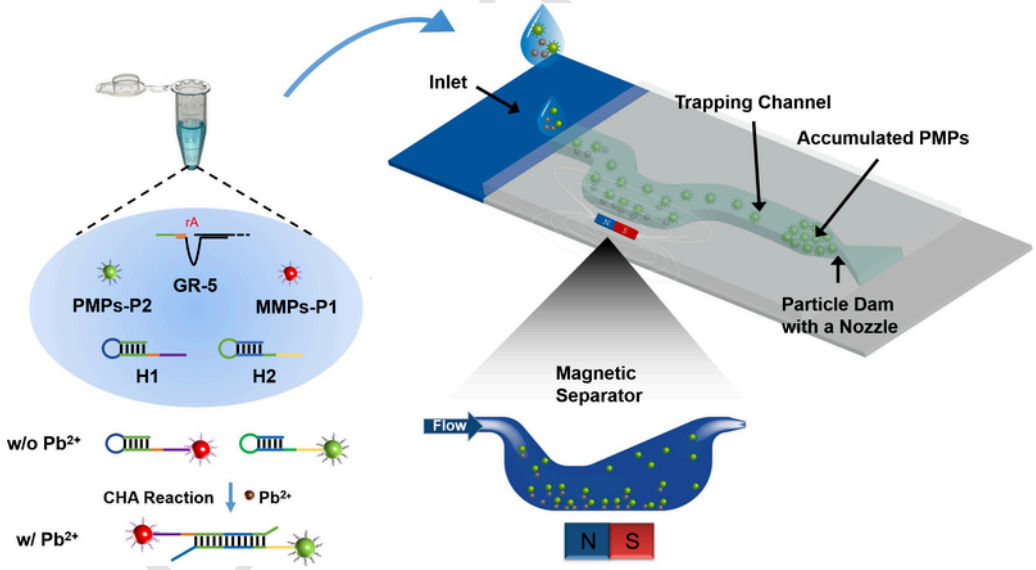

Fig. 3. Working principle of the microfluidic device. After CHA and reaction with microparticles, the solution is loaded to a microfluidic device driven by capillary flow. A magnetic separator would first capture the MMPs and MMPs-H1H2-PMPs, and free PMPs can continue flowing until be trapped by a particle dam. Therefore, more lead ions would cause shorter PMP accumulation with a length readable by the naked eye.

2. Materials and methods

2.1. Oligonucleotide Sequences

The sequences of GRDS (Integrated DNA Technologies) and other oligonucleotides (BGI BIO-Solutions HONGKONG Co., Ltd.) are listed in Table S1. They were received in powder state and dissolved in diethyl pyrocarbonate (DEPC) -treated water (Thermo Fisher Scientific) at 100 μM. GRDS hybridizes with GRE to form the GR-5, which is cleaved by lead ions and releases a short sequence T (underlined sequence of GRDS) (Fig. S1) [55]. As such, the H1 was designed as a hairpin with stem part (labelled bold in Table S1), which can hybridize with the T (via the sequence labelled italic), and its opened form can then hybridize with H2 (via the sequence of H1 and H2 labelled underline). Thus, the stem part of H2 (the sequence labelled bold) can be opened and displace the T. Meanwhile, biotinylated P1 and P2 immobilized on streptavidin-coated MMPs and streptavidin-coated PMPs can hy-

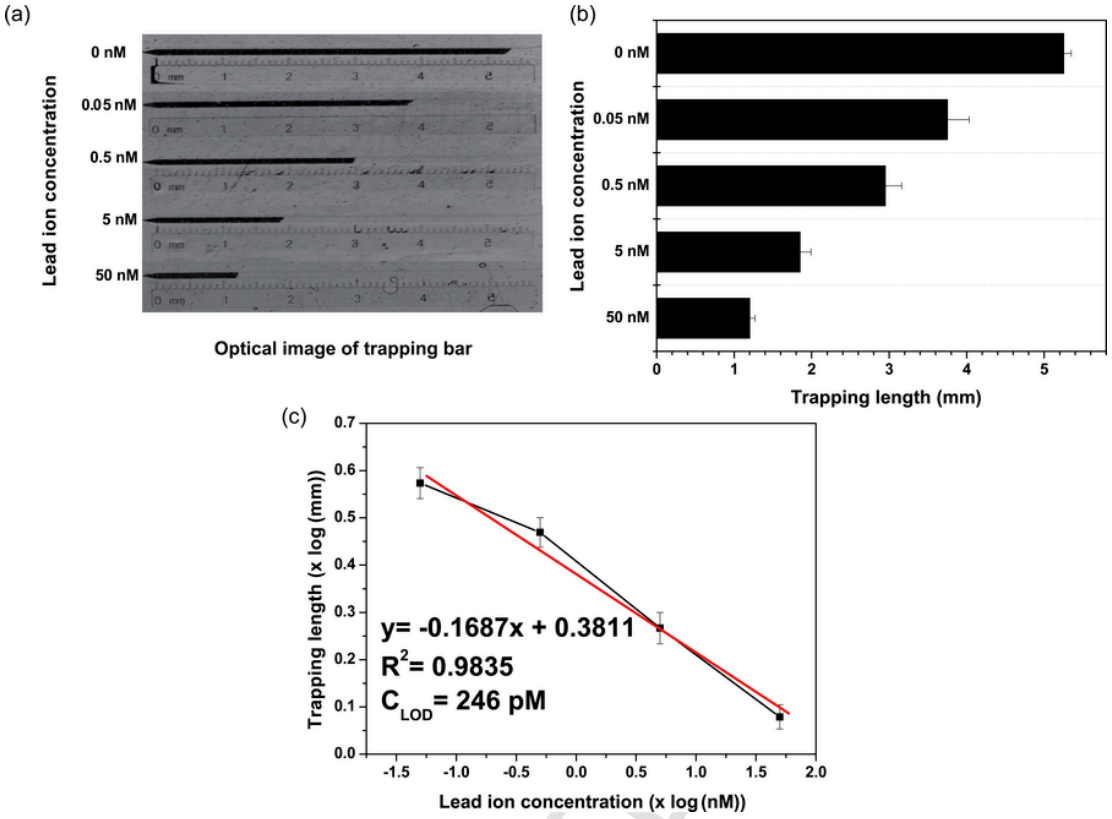

Fig. 4. LOD of lead detection using the microfluidic device. (a) Optical Image of accumulating PMP with respect to Pb^{2+} concentration. (b) The measured PMP accumulation length. (c) The linear regression of the PMP accumulation length with respect to Pb^{2+} concentration (mean ± max deviation, n = 3).

bridize with the spare space of H1 and H2, respectively, leading to the formation of MMPs-H1H2-PMPs.

2.2. Agarose Gel Electrophoresis

First, 100 mL of 1X TAE buffer (Thermo Fisher Scientific) was used to dissolve 4 g of agarose powder (Thermo Fisher Scientific). The mixture was boiled in micro-wave oven for 2 min, followed by addition of 4 µl of 10,000X GelRed® Nucleic Acid Gel Stain (Biotium) and boiling for another 2 min. Next, all the solution was transferred to a casting tray and cooled down for 30 min in room temperature to form 4% agarose gel, and then placed in the gel tank filled with 1X TAE buffer. The concentration of all oligonucleotide strands and Pb^{2+} was 200 nM in binding buffer (50 mM Tris-HCl, 140 mM NaCl, 5 mM KCl, pH 7.5, all from Sigma-Aldrich, USA). Before loading into the electrophoresis unit, each sample was mixed with 6X DNA Gel Loading Dye (Thermo Fisher Scientific) with a ratio of 5:1. The electrophoresis was conducted under 130 V for 40 min using GeneRuler Ultra Low Range DNA Ladder (SM1211, Thermo Fisher Scientific) as the reference. Finally, BIO-RAD Gel Doc EZ Imager was used to visualize the result.

2.3. Modification of Microparticles

Based on the streptavidin-biotin bonds, MMPs and PMPs were modified with P1 and P2, respectively. For magnetophoresis assay, 3.5 µL of MMPs (CME0101, 0.86 µm in diameter, 1.827×10^{10} microspheres/mL, Bangs Laboratories, Inc., USA) was mixed with 3.5 µL of P1 (100 µM), while 3.5 µL of PMPs (CP01004, 0.989 µm in diameter, 1.557×10^{10} microspheres/mL, Bangs Laboratories, Inc., USA) was mixed with 3.5 µL of P2 (100 µM). For particles used in microfluidic chip, 5 µL of MMPs (CMC0100, 0.36 µm in diameter, 3.063×10^{11} microspheres/mL, Bangs Laboratories, Inc., USA) was mixed with 5 µL of P1 (100 µM), while 5 µL of PMPs (CP01008, 15.34 µm in diameter, 5.033×10^{6} microspheres/mL, Bangs Laboratories, Inc., USA) was mixed with 5 µL of P2 (100 µM). The mixed solution was gently shaken for 30 minutes to immobilize the biotinylated oligonucleotides on the streptavidin-coated microparticles. Next, the microspheres were rinsed 3 times respectively with 200 µL of washing buffer (50 mM Tris-HCl, 140 mM NaCl, 5 mM KCl, 0.2% Tween 20, pH 7.5, all from Sigma-Aldrich, USA) to remove the excess oligonucleotides. In the washing step, MMPs were separated and collected by a magnet rack, and PMPs were separated and collected by a centrifuge (13.8 × g, 5 minutes). Finally, for magnetophoresis assay, P1 modified MMPs and P2 modified PMPs were adjusted to 3.5 µL (10 mg/mL (1% solids w/v)); for microfluidic chip, P1 modified MMPs and P2 modified PMPs were adjusted to 5 µL (10 mg/mL (1% solids w/v)).

2.4. Lead-Mediated Cleavage of GR-5 with CHA Amplification

One µM of GRDS and GRE were incubated in binding buffer (50 mM Tris-HCl, 140 mM NaCl, 5 mM KCl, pH 7.5) for 30 min to form 1 µM GR-5. Next, 100 or 200 nM of GR-5 in 2 µL (diluted in binding buffer) was mixed with 2 µL of lead ion solution, i.e. lead (II) acetate trihydrate powder (Strem Chemicals, Inc.) diluted in Deionized (DI) water (Milli-Q Plus system, with a resistivity of 18.2 MΩ cm) at different concentration together with 5 µL binding buffer and incubated for another 30 min. To test the selectivity, the lead solution was replaced by 2 µL of Barium (Ba^{2+}), Mercury (Hg^{2+}), Copper (Cu^{2+}), Strontium (Sr^{2+}), Cadmium (Cd^{2+}), Manganese (Mn^{2+}), Cobalt (Co^{2+}), Nickel (Ni^{2+}), and Calcium (Ca^{2+}) solution (AA standard form, J&K Scientific). For reaction with different pH values, lead solution was prepared in DI water with different pH values by adding NaOH/HCl. For reaction with different water hardness, lead solution was prepared in 4 kinds of water samples from different brands of bottled water with varied hardness. Classification of water hardness is based on WQA (Water Quality Association), which defines the water hardness using American de-

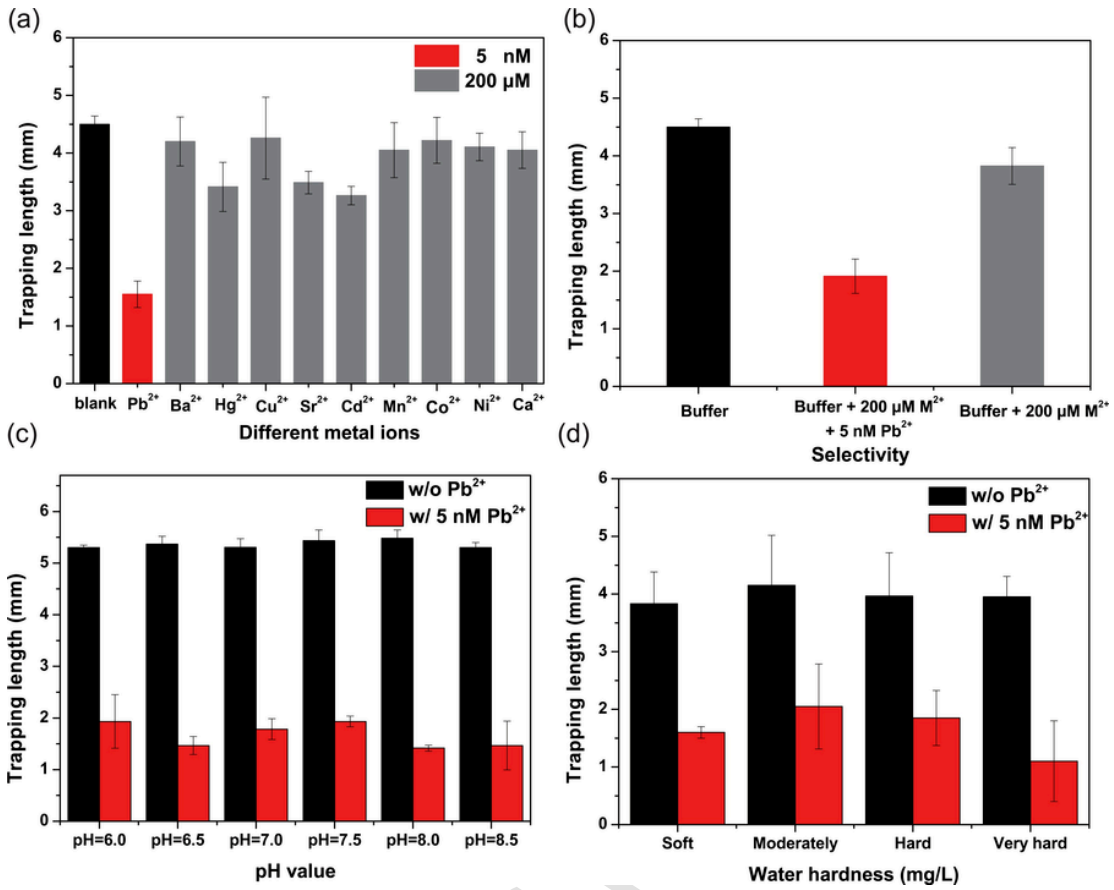

Fig. 5. Detection with environmental interference. (a) Selectivity of lead ion detection against other nine metal ions. (b) Selectivity of lead ion detection in a cocktail of other nine metal ions (Pb^{2+}: addition of Pb^{2+} (5 nM); M^{2+}: addition of all other nine ions (200 μM) except Pb^{2+}; Buffer: blank sample). (c) Tolerance of pH range from 6.0 to 8.5. (d) Tolerance of different water hardness levels at 55 mg/L (Soft), 107.5 mg/L (Moderately Hard), 157.7 mg/L (Hard), and 318.3 mg/L (Very Hard) (mean ± max deviation, n = 3).

gree equivalent to mg/L by the equation of Water hardness (mg/L) = Ca (mg/L) × 2.497 + Mg (mg/L) × 4.118. Accordingly, the water hardness is calculated as 55 mg/L from Bourbon™ (soft), 107.5 mg/L FIJI™ (moderately hard), 157.7 mg/L from AQUA™ (hard), and 318.3 mg/L from Vittel™ (very had). For tests in tap water, 2 μL of lead ions was first spiked in 98 μL of tap water to make the final concentration at 50 nM. Next, 2 μL of tap water with or without spiked lead was used to mixed with GR-5 solution as aforementioned. For tests in blood, 2 μL of lead ions was also first spiked in 98 μL of whole blood (sheep blood, Nanjing Maojie Microorganism Technology Co., Ltd) or plasma (supernatant after centrifugation 13.8 × g for 45 min) to make the final concentration at 0, 0.1 nM, 1 nM, 10 nM (for plasma), 100 nM, 1 μM, and 10 μM. Next, 2 μL of blood with or without spiked lead was mixed with the GR-5 solution. For all above, after the hydrolytic reaction with GR-5 for 30 min, 9 μL of product solution (containing 2 μL of 100 nM GR-5, 2 μL of metal ions at different concentration in binding buffer, water hardness samples, tap water, whole blood, or plasma and 5 μL of binding buffer) was mixed with 100 nM of H1 and H2 in 4 μL in binding buffer and incubated 30 min for CHA-based signal amplification.

2.5. Magnetophoresis Assay

After hydrolytic reaction of GR-5 and CHA amplification, the 13 μL of product solution in binding buffer, water hardness samples, or tap water was mixed with MMPs-P1 and PMPs-P2 (3.5 μL, 10 mg/mL) and incubated 30 min with gentle shaking to form the MMPs-H1H2-PMPs sandwich structure. For detection in whole blood or plasma, MMPs-P1 (3.5 μL, 10 mg/mL) was first added and incubated for 30 min. After rinsing by washing buffer for 3 times to remove the blood cells and plasma, the solution volume was adjusted to 16.5 μL using binding buffer, and PMPs-P2 (3.5 μL, 10 mg/mL) was then added and incubated for 30 min. Next, the MMPs-H1H2-PMPs were removed by a magnetic rack, and the turbidity of supernatant with free PMPs was observed by the naked eye, or quantified by absorbance measurement using UV-Vis spectrometer (BioDrop μLITE, UK).

2.6. Design and Fabrication of Microfluidic Chip

The layout of the microfluidic device is based on our previous design [41,55]. Norland optical adhesive 63 (NOA63, Norland Products, USA) is used as the channel material because plasma treatment (Harrick Plasma, 400 mTorr, 2 min) enables the bonding to glass substrate while maintaining prolonged hydrophilic property for many days, thus eliminating the hydrophobicity recovery issue as compared to commonly used polydimethylsiloxane (PDMS). The fabrication starts from spin-coating SU8 2015 photoresist (Gersteltec Sarl, Switzerland) onto a silicon wafer (Suzhou Crystal Silicon Electronic & Technology Co., Ltd.) at 1200 rpm. After UV exposure and development, a SU8 master with a thickness of 25 ± 0.3 μm was obtained. Next, the SU8 master was poured with PDMS precursor (elastomer base: curing agent = 10:1, SylgardTM 184, Dow Corning, USA) and baked at 70 °C for 2 h. After being cured and peeled off, the patterned surface of the PDMS was treated with plasma (Harrick Plasma, 400 mTorr, 2 min) before application of (3-Aminopropyl) trimethoxysilane (Sigma Aldrich, USA) by gas-phase deposition at room temperature for 6 h. Afterward, a secondary PDMS casting was performed on the patterned surface of the first PDMS. The uncured NOA63 glue was smeared onto the patterned surface of the secondary PDMS, and covered by a commercially avail-

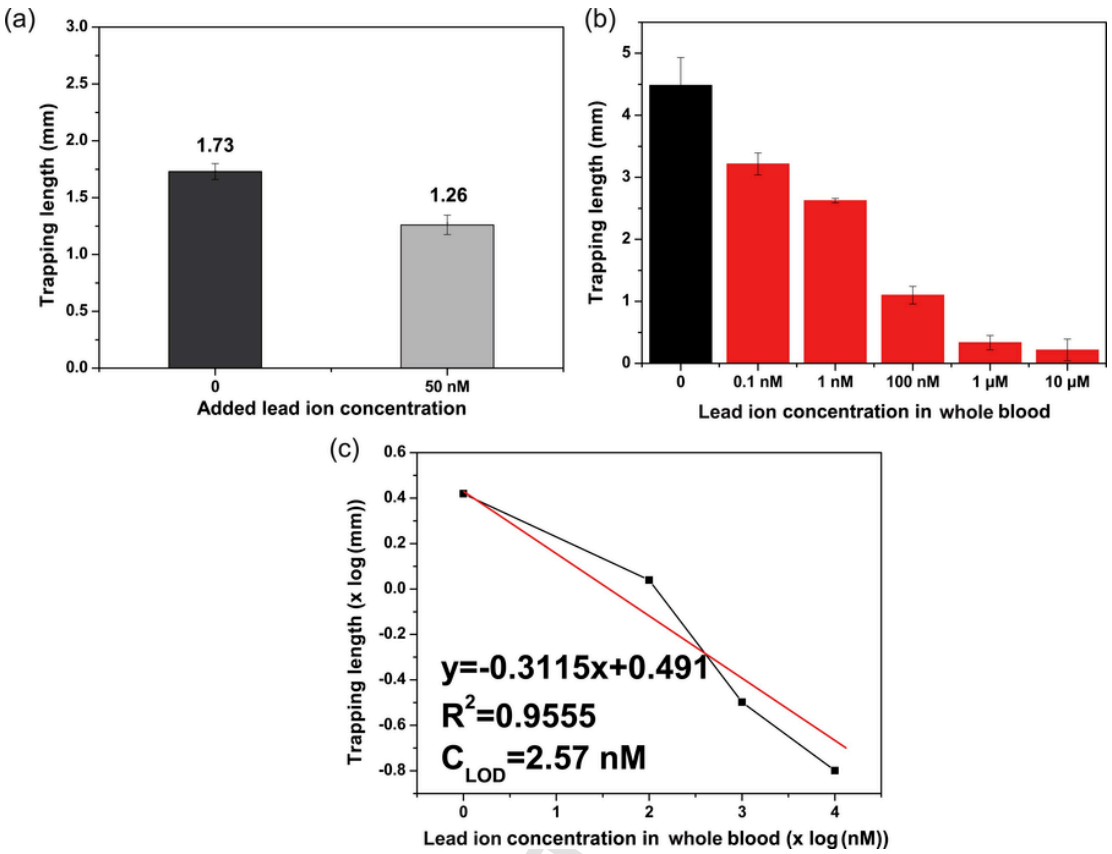

Fig. 6. Application in tap water and whole blood. (a) Lead detection in tap water. (b) Detection in whole blood with spiked lead ions. (c) The linear regression of the PMP accumulation length with respect to Pb^{2+} concentration in whole blood (mean ± max deviation, n = 3).

Table 2
Lead detection in tap water

	Original Pb^{2+} (nM)	Spiked Pb^{2+} (nM)	Found (nM)	Recovery (%)
Tap water 1	8.68	0	7.05 ± 1.72	81.2
Tap water 2	8.68	50	46.14 ± 16.46	78.6

able polypropylene film (KOKUYO, Japan) with 100 μm thickness. After expose to UV-light for 50 seconds, the NOA can be peeled-off easily. Before bonding, trichloro (1H, 1H, 2H, 2H-perfluorooctyl) silane (97%) (J&K Scientific Ltd.) diluted in toluene (10 wt%) was used to coat a glass slide inside a vacuum chamber for 40 min. After coating, a tape was used to cover the outer region of the inlet to protect its hydrophobicity. Next, plasma treatment (Harrick Plasma, 800 mTorr, 2 min) was applied to the unprotected region of the glass slide and the patterned surface of NOA63, allowing bonding the NOA63 chip onto the glass slide. As such, the microfluidic device can maintain inner wall of NOA63 microchannel hydrophilic as opposed to the hydrophobic outer region of the inlet. Finally, a neodymium magnet in the size of 2.6 mm × 1.8 mm × 1.5 mm was then glued at 1 mm next to the magnetic separator.

2.7. Detection in Microfluidic Chip

The procedure for hydrolytic reaction of GR-5 and CHA amplification was the same as aforementioned. After that, for detection in binding buffer, water hardness samples, or tap water, 1 μL of solution extracted from the 13 μL of product solution (containing 2 μL of 200 nM GR-5, 2 μL of metal ions solution, 4 μL of 200 nM H1 and H2 mixed solution, and 5 μL of binding buffer) was mixed with 1 μL of MMPs (10 mg/mL) and 1 μL of PMPs (10 mg/mL) for 30 min incubation with gentle shaking. For detection in whole blood / plasma, 1 μL solution extracted from the 13 μL of product solution was mixed with 1 μL of MMPs (10 mg/mL) for 30 min incubation with gentle shaking. After rinsing for 3 times to remove the blood cells and plasma, the solution volume was brought to 2 μL with washing buffer. Next, 1 μL PMPs (10 mg/mL) was added and incubate for another 30 min with gentle shaking. At last, 3 μL final solution was loaded on the microfluidic chip. All the steps were carried out at room temperature.

3. Results and discussion

We first design the CHA triggered by the released T after hydrolytic cleavage of GR-5 DNAzyme (Fig. 1). The system involves two hairpin structures, H1 and H2. At beginning, GR-5 is cleaved by lead ions to release the oligonucleotide Target (T) (Fig. S1), which hybridizes with H1 and opens its hairpin structure. Next, the opened H1 can subsequently open the H2 and then displace and release the T, which can then open another H1 for the next cycle. After repeating, it produces massive amount of assembled H1 and H2 which can hybridize the biotinylated oligonucleotides P1 and P2 on streptavidin-coated MMPs and PMPs, respectively, leading to the formation of MMPs-H1H2-PMPs complex.

Agarose gel electrophoresis was used to ensure the hydrolytic reaction of DNAzyme and CHA. Our results showed that the GR-5 was formed by pairing GRE with GRDS (well 1-3 in Fig. S2), and cleaved by Pb^{2+} to release the T (well 4 in Fig. S2). Before encountering the T, the H1 and H2 can coexist stably (well 5-7 in Fig. S2). However, when T was released, it can hybridize with H1 (well 8 in Fig. S2), followed

by the formation of H1H2 complex (upper band of well 9 in Fig. S2) by recycling the T during each cycle.

Next, magnetophoresis was used to optimize the concentration of H1 and H2 for effective connection between MMPs and PMPs. MMPs with P1 and PMPs with P2 are added following the hydrolytic reaction of GR-5 and CHA (Fig. 1). After formation of MMPs-H1H2-PMPs, an external magnetic field is applied, which pulls MMPs and MMPs-H1H2-PMPs to the sidewall of a test tube, leaving only PMPs freely suspending in the solution [55,56]. As the amount of free PMPs is inversely proportional to the number of MMPs-H1H2-PMPs, more lead would make the solution clear because of the reduced Mie scattering and solution turbidity. In contrast, if MMPs and PMPs are not connected, only MMPs would be attracted and the solution remains turbid. Using the amount and ratio of MMPs and PMPs optimized previously [57], different concentrations of H1 and H2 were tested, and the solution turbidity was measured by UV-Vis spectrometry (Fig. S3). By comparing the signal-to-noise ratios, 20 nM of H1 and H2 was selected as the optimized concentration (in the final solution with GR-5, Pb^{2+}, H1, H2, MMPs, and PMPs).

Notably, with the use of CHA, it is possible to achieve complete transparency with only very few of the liberated target if the reaction time is long enough. However, long reaction time is impractical even though lower LOD may be obtained. To balance it, the incubation time for CHA was studied. Using lead ions with different concentration (0, 0.05 nM and 50 nM), the absorbance decreased with the increase of CHA reaction time (Fig. S4). Importantly, we found that 30 min of CHA reaction is already sufficient to discriminate the samples with the lowest concentration of lead, 0.05 nM, from the blank control. Therefore, to minimize the required reaction time, 30 min was chosen as the optimal time for CHA reaction.

The LOD was explored based on such magnetophoretic assay with various Pb^{2+} concentrations from 0 to 50 nM (total volume: 20 μl). When Pb^{2+} was absent (0 M), the solution was completely turbid and opaque. On the contrary, along with the increment of Pb^{2+} concentration, the suspension gradually became clear and transparent. The distinction can be differentiated by the naked eye when Pb^{2+} was beyond 4 nM (Fig. 2a). UV-Vis spectrometer was applied to measure the spectral absorbance of the supernatant (Fig. 2b and c). As expected, the absorbance was inversely proportional to the concentration of Pb^{2+} with a linear range of 50 pM – 2 nM ($R^2 = 0.997$, Fig. 2d). On basis of the absorbance at 400 nm, the LOD was 472 pM (estimated based on 3 σ/k, where k represents the absolute slope of the linear regression equation, and σ represents the standard deviation of the blank sample).

Next, a microfluidic device was used to explore the visual and quantitative detection (Fig. 3). Once the MMPs-H1H2-PMPs are formed, the microparticle solution is loaded into a microfluidic device consisting of an inlet for the sample loading, a stomached-shape magnetic separator, a trapping channel, and a particle dam with a narrowing nozzle. The inlet contains a hydrophobic outer region to ensure all microparticle solution can wick into the hydrophilic microchannel after loading. The solution first passes the magnetic separator that attracts the MMPs and MMPs-H1H2-PMPs to the side, leaving free PMPs to continue flowing until being trapped at a particle dam because the PMP diameter (15.34 μm) is wider than the narrowest nozzle width. As such, PMPs would accumulate in the trapping channel and form a visual bar with a length inversely proportional to the amount of lead ions and quantifiable by the naked eye.

To determine the LOD based on PMP accumulation in the microfluidic device, various concentrations of Pb^{2+} (0, 0.05, 0.5 and 50 nM) were tested. As shown in Fig. 4a, shorted length of PMP accumulation with the increased Pb^{2+} concentration can be easily observed by the naked eye. According to the trapping length and lineage regression (Fig. 4b and c), a limit of detection of 246 pM was determined, which is around 300-fold lower than the permitted concentration, 72.4 nM, according to EPA.

Notably, this LOD is much lower than that of our previous method, i.e. 2.12 nM [41]. There are two reasons. First, the particle connection is changed from "turn-off" to "turn-on" mechanism. Previously GR-5 was used to connect MMPs and PMPs, and cleaved when Pb is present, causing more PMPs accumulation in the particle dam. While this is a simple way to report signals, more lead is needed to break the already-formed particle-particle connections. In contrast, our current method is based on newly-formed connections triggered by the presence of lead. As such, less lead is needed, making the detection more sensitive when lead concentration is low. Second, instead of directly affecting the particle connections, the released T from GR-5 after lead-mediated cleavage is used to trigger the CHA amplification. Thus, small amount of T can lead to mass-produced hairpin assembly H1H2 connecting MMPs and PMPs. As a result, the sensitivity of Pb^{2+} detection has been dramatically improved.

To explore the selectivity of lead detection, different metal ions including Barium (Ba^{2+}), Mercury (Hg^{2+}), Copper (Cu^{2+}), Strontium (Sr^{2+}), Cadmium (Cd^{2+}), Manganese (Mn^{2+}), Cobalt (Co^{2+}), Nickel (Ni^{2+}), and Calcium (Ca^{2+}) were applied. The magnetophoresis assay showed that lead at 10 nM can greatly reduce the solution turbidity (Fig. S5a), indicating the successful formation of MMPs-H1H2-PMPs. However, such connection was not observed with other more concentrated metal ions (400 μM) as the solution remained turbid. Consistently, the high selectivity was again observed by detecting Pb^{2+} in a cocktail solution of other nine metal ions (Fig. S5b). Similar results were obtained on microfluidic device. The trapping length was about 1.5 mm when Pb^{2+} was 5 nM (Fig. 5a). However, for other nine metal ion samples with much higher concentration (200 μM), the length of PMP accumulation was much longer and similar to the length of the blank control (without Pb^{2+}). Again, the selectivity can be observed in a cocktail solution containing Pb^{2+} (5 nM) with all other nine metal ions (200 μM) (Fig. 5b). Thus, the selectivity to lead detection is more than 40,000-folds against other metal ions according to the concentration of use. The superior selectivity is attributed to the property of GR-5. GR-5 is the first DNAzyme isolated through in vitro selection specific to Pb^{2+} [58]. Compared to other DNAzyme, GR-5 contains catalytic core regions for Pb^{2+}-dependent activity while excluding other peripheral motifs active with other divalent metal ions [59]. Therefore, only Pb^{2+} led to an obvious decrease of absorbance and trapping length under the same conditions against other metal ions.

Moreover, the stability and tolerance of the detection to various water sources with different acidity/basicity and hardness were investigated. Five nM Pb^{2+} were added in water with pH = 6.0, 6.5, 7.0, 7.5, 8.0, and 8.5 or water samples with different hardness levels. For pH value in the tested range (Fig. 5c), the results maintain equable, indicating the tolerance of different water sources with wide pH range. For four water samples with different hardness scale (Fig. 5d), distinction of trapping length was observed between samples with/without 5 nM Pb^{2+}, suggesting the excellent tolerance to water hardness. Also, the result was reconfirmed by measuring the solution absorbance using magnetophoresis assay (Fig. S5c and d).

Finally, tap water and whole blood were applied with spiked lead ions. ICP-MS shows that the tap water contains 8.68 nM of Pb^{2+}. The PMP trapping length was 1.73 ± 0.28 mm observed from the device (Fig. 6a), which can be calculated as 7.05 ± 1.72 nM using the linear equation in Fig. 4c. Thus, 81.2% of recovery rate was obtained (Table 2). Furthermore, such high recovery rate can be again achieved by spiking additional 50 nM Pb^{2+} in the tap water (78.6%, Table 2). To explore the compatibility with diagnosis of lead intoxication, blood with spiked Pb^{2+} was applied. First, blood plasma was tested because it is a stable and standard matrix in many clinic assays. Although the sensitivity was reduced, a LOD of 16.02 nM can still be achieved in such complex biofluids (Fig. S6). Furthermore, considering the application in resource-limited settings without a centrifuge or even electricity, unprocessed whole blood was tested. Strikingly, a LOD of 2.57 nM (Fig. 6b and c) was still achieved, which is around 100 times

lower than the upper limit for blood lead for child, 241.3 nM (5 μg/dL), recommended by the Centers for Disease Control (US). The sensitivity is even better than detection in blood plasma possibly because of the exemption of centrifugation. Together, it demonstrates that the microfluidic device is compatible with complex biofluids, and retains high sensitivity without additional blood purification process, indicating its potential for future practical application.

4. Conclusions

Using cascade-amplified microfluidic particle accumulation, we report an enzyme-free, label-free, and highly sensitive method for visual quantitative detection of lead ions. The hydrolytic cleavage of GR-5 and CHA can be conducted in room temperature without time consuming thermal cycling. By rapid PMP accumulation as a visually quantitative readout in the capillary-driven microfluidic device, the method achieved LOD at 246 pM, and is extremely selective (> 40,000 folds to other metal ions), and highly tolerant to acidity/basicity (6 – 8.5) and water hardness. Such performance is much better than other miniaturized platform with visual readouts. More importantly, this detection can be applied to detect lead in tap water with high recovery rate (> 78%) and in whole blood with LOD of 2.57 nM, providing a simple and convenient device for monitoring water safety and lead intoxication.

CRediT authorship contribution statement

Minghui Wu: Conceptualization, Methodology, Investigation, Writing - original draft. **Gaobo Wang:** Methodology, Investigation, Formal analysis. **Lok Ting Chu:** Methodology, Formal analysis. **Hanjin Huang:** Investigation. **Ting-Hsuan Chen:** Conceptualization, Supervision, Funding acquisition, Project administration, Writing - review & editing.

Declaration of Competing Interest

The authors declare no conflict of interest.

Acknowledgements

We are pleased to acknowledge the funding support from City University of Hong Kong (6000720 and 9667161) and the Research Grant Council, University Grants Committee (no. N_CityU119/19, 11217217, and 11277516).

Appendix A. Supplementary data

Supplementary material related to this article can be found, in the online version, at doi:https://doi.org/10.1016/j.snb.2020.128727.

References

[1] D. Yang, X. Liu, Y. Zhou, L. Luo, J. Zhang, A. Huang, et al., Aptamer-based biosensors for detection of lead(ii) ion: a review, Anal. Methods 9 (2017) 1976–1990.

[2] P. Mladenka, L. Applova, J. Patocka, V.M. Costa, F. Remiao, J. Pourova, et al., Comprehensive review of cardiovascular toxicity of drugs and related agents, Med. Res. Rev. 38 (2018) 1332–1403.

[3] CDC Response to Advisory Committee on Childhood Lead Poisoning Prevention Recommendations in "Low Level Lead Exposure Harms Children: A Renewed Call of Primary Prevention", CDC Response to Advisory Committee on Childhood Lead Poisoning Prevention Recommendations in "Low Level Lead Exposure Harms Children: A Renewed Call of Primary Prevention" https://www.cdc.gov/nceh/lead/acclpp/cdc_response_lead_exposure_recs.pdf. (2012, July).

[4] S. Adrienne, S. Ettinger, A.G. Wengrovitz, Guidelines for the identification and management of lead exposure in pregnant and lactating women, 2010.

[5] S. Mustafa, U.K. Aslıhan, E. Latif, D. Mehmet, Column Preconcentration/Separation and Atomic Absorption Spectrometric Determinations of Some Heavy Metals in Table Salt Samples Using Amberlite XAD-1180, Turk. J. Chem. 27 (2003) 235–242.

[6] C. Yong, M. Sugunya, J. Rudolf, D.J. Ronald, Gas chromatographic determination of organomercury following aqueous derivatization with sodium tetraethylborate and sodium tetraphenylborate Comparative study of gas chromatography coupled with atomic fluorescence spectrometry, atomic emission spectrometry and mass spectrometry, J. Chromatogr. A 876 (2000) 147–155.

[7] A.A. Ammann, Inductively coupled plasma mass spectrometry (ICP MS): a versatile tool, J. Mass. Spectrom. 42 (2007) 419–427.

[8] Y. Ge, Y. Guo, W. Qin, Polyamidoamine dendrimers as sweeping agent and stationary phase for rapid and sensitive open-tubular capillary electrophoretic determination of heavy metal ions, Talanta 121 (2014) 50–55.

[9] L. Jinping, Y. Hsieh, W. Donald, N. Milos, Design of 3-(4-Carboxybenzoyl)-2-quinolinecarboxaldehyde as a Reagent for Ultrasensitive Determination of Primary Amines by Capillary Electrophoresis Using Laser Fluorescence Detection, Anal. Chem. 63 (1991) 408–412.

[10] Y. Zang, J. Lei, Q. Hao, H. Ju, "Signal-on" photoelectrochemical sensing strategy based on target-dependent aptamer conformational conversion for selective detection of lead(II) ion, ACS Appl. Mater. Interfaces 6 (2014) 15991–15997.

[11] D. Nie, H. Wu, Q. Zheng, L. Guo, P. Ye, Y. Hao, et al., A sensitive and selective DNAzyme-based flow cytometric method for detecting Pb^{2+} ions, Chem. Commun. (Camb) 48 (2012) 1150–1152.

[12] S. Gui, Y. Huang, Y. Zhu, Y. Jin, R. Zhao, Biomimetic Sensing System for Tracing Pb(2+) Distribution in Living Cells Based on the Metal-Peptide Supramolecular Assembly, ACS. Appl. Mater. Interfaces 11 (2019) 5804–5811.

[13] T. Zhang, C. Liu, W. Zhou, K. Jiang, C. Yin, C. Liu, et al., Ultrasensitive Detection of Pb(2+) Based on a DNAzyme and Digital PCR, J. Anal. Methods Chem. 2019 (2019) 1–6.

[14] H.B. Wang, L. Wang, K.J. Huang, S.P. Xu, H.Q. Wang, L.L. Wang, et al., A highly sensitive and selective biosensing strategy for the detection of Pb^{2+} ions based on GR-5 DNAzyme functionalized AuNPs, New J. Chem. 37 (2013) 2557–2563.

[15] J. Kosman, B. Juskowiak, Peroxidase-mimicking DNAzymes for biosensing applications: a review, Anal. Chim. Acta. 707 (2011) 7–17.

[16] H. Liu, Y. Chen, C. Song, G. Tian, S. Li, G. Yang, et al., Novel and label-free colorimetric detection of radon using AuNPs and lead(II)-induced GR5 DNAzyme-based amplification strategy, Anal. Bioanal. Chem. 410 (2018) 4227–4234.

[17] T. Fu, S. Ren, L. Gong, H. Meng, L. Cui, R.M. Kong, et al., A label-free DNAzyme fluorescence biosensor for amplified detection of Pb^{2+}-based on cleavage-induced G-quadruplex formation, Talanta 147 (2016) 302–306.

[18] X. Li, G. Wang, X. Ding, Y. Chen, Y. Gou, Y. Lu, A "turn-on" fluorescent sensor for detection of Pb2+ based on graphene oxide and G-quadruplex DNA, Phys. Chem. Chem. Phys. 15 (2013) 12800–12804.

[19] R. Metivier, I. Leray, B. Valeur, A highly sensitive and selective fluorescent molecular sensor for Pb(II) based on a calix[4]arene bearing four dansyl groups, Chem. Commun. (Camb) (2003) 996–997.

[20] X. Niu, Y. Zhong, R. Chen, F. Wang, Y. Liu, D. Luo, A "turn-on" fluorescence sensor for Pb^{2+} detection based on graphene quantum dots and gold nanoparticles, Sens. Actuators, B 255 (2018) 1577–1581.

[21] S. Pang, S. Liu, X. Su, An ultrasensitive sensing strategy for the detection of lead (II) ions based on the intermolecular G-quadruplex and graphene oxide, Sens. Actuators, B 208 (2015) 415–420.

[22] A. Ravikumar, P. Panneerselvam, K. Radhakrishnan, Fluorometric determination of lead(II) and mercury(II) based on their interaction with a complex formed between graphene oxide and a DNAzyme, Microchim. Acta 185 (2017) 1–8.

[23] D. Zhang, R. Fu, Q. Zhao, H. Rong, H. Wang, Nanoparticles-free fluorescence anisotropy amplification assay for detection of RNA nucleotide-cleaving DNAzyme activity, Anal. Chem. 87 (2015) 4903–4909.

[24] X.H. Zhao, R.M. Kong, X.B. Zhang, H.M. Meng, W.N. Liu, W. Tan, et al., Graphene-DNAzyme based biosensor for amplified fluorescence "turn-on" detection of Pb^{2+} with a high selectivity, Anal. Chem. 83 (2011) 5062–5066.

[25] H. Cui, X. Xiong, B. Gao, Z. Chen, Y. Luo, F. He, et al., A Novel Impedimetric Biosensor for Detection of Lead (II) with Low-cost Interdigitated Electrodes Made on PCB, Electroanalysis 28 (2016) 2000–2006.

[26] Y. Wang, J. Irudayaraj, A SERS DNAzyme biosensor for lead ion detection, Chem. Commun. (Camb) 47 (2011) 4394–4396.

[27] X. Yi, A.R. Aaron, W.P. Kevin, Electrochemical Detection of Parts-Per-Billion Lead via an Electrode-Bound DNAzyme Assembly, J. Am. Chem. Soc. 129 (2007) 262–263.

[28] Y. Zhang, S. Xiao, H. Li, H. Liu, P. Pang, H. Wang, et al., A Pb^{2+}-ion electrochemical biosensor based on single-stranded DNAzyme catalytic beacon, Sens. Actuators, B 222 (2016) 1083–1089.

[29] A. Gao, C.X. Tang, X.W. He, X.B. Yin, Electrochemiluminescent lead biosensor based on GR-5 lead-dependent DNAzyme for Ru(phen)3(2+) intercalation and lead recognition, Analyst 138 (2013) 263–268.

[30] M. Zhang, L. Ge, S. Ge, M. Yan, J. Yu, J. Huang, et al., Three-dimensional paper-based electrochemiluminescence device for simultaneous detection of Pb^{2+} and Hg^{2+} based on potential-control technique, Biosens. Bioelectron. 41 (2013) 544–550.

[31] Y. Zhang, L. Zhang, Q. Kong, S. Ge, M. Yan, J. Yu, Electrochemiluminescence of graphitic carbon nitride and its application in ultrasensitive detection of lead(II) ions, Anal. Bioanal. Chem. 408 (2016) 7181–7191.

[32] L. Beqa, A.K. Singh, S.A. Khan, D. Senapati, S.R. Arumugam, P.C. Ray, Gold nanoparticle-based simple colorimetric and ultrasensitive dynamic light scattering assay for the selective detection of Pb(II) from paints, plastics, and water samples, ACS Appl. Mater. Interfaces 3 (2011) 668–673.

[33] B. Chen, Z. Wang, D. Hu, Q. Ma, L. Huang, C. Xv, et al., Scanometric nanomolar lead (II) detection using DNA-functionalized gold nanoparticles and silver stain enhancement, Sens. Actuators, B 200 (2014) 310–316.

[34] P. Chen, R. Zhang, Q. Jiang, X. Xiong, S. Deng, Colorimetric Detection of Lead Ion Based on Gold Nanoparticles and Lead-Stabilized G-Quartet Formation, J. Biomed. Sci. Eng. 08 (2015) 451–457.

[35] L. Juewen, L. Yi, Accelerated Color Change of Gold Nanoparticles Assembled by DNAzymes for Simple and Fast Colorimetric Pb^{2+} Detection, J. Am. Chem. Soc. 126 (2004) 12298–12305.
[36] L. Juewen, L. Yi, A Colorimetric Lead Biosensor Using DNAzyme-Directed Assembly of Gold Nanoparticles, J. Am. Chem. Soc. 125 (2003) 6642–6643.
[37] S. Thatai, P. Khurana, S. Prasad, S.K. Soni, D. Kumar, Trace colorimetric detection of Pb^{2+} using plasmonic gold nanoparticles and silica–gold nanocomposites, Microchem. J. 124 (2016) 104–110.
[38] D. Mazumdar, J. Liu, G. Lu, J. Zhou, Y. Lu, Easy-to-use dipstick tests for detection of lead in paints using non-cross-linked gold nanoparticle-DNAzyme conjugates, Chem. Commun. (Camb) 46 (2010) 1416–1418.
[39] C. Fan, S. He, G. Liu, L. Wang, S. Song, A portable and power-free microfluidic device for rapid and sensitive lead (Pb2+) detection, Sensors (Basel) 12 (2012) 9467–9475.
[40] X. Liu, Y. Wang, Y. Song, Visually multiplexed quantitation of heavy metal ions in water using volumetric bar-chart chip, Biosens. Bioelectron. 117 (2018) 644–650.
[41] G. Wang, L.T. Chu, H. Hartanto, W.B. Utomo, R.A. Pravasta, T.H. Chen, Microfluidic Particle Dam for Visual and Quantitative Detection of Lead Ions, ACS Sens. 5 (2020) 19–23.
[42] Z. Huang, J. Chen, Z. Luo, X. Wang, Y. Duan, Label-Free and Enzyme-Free Colorimetric Detection of Pb(2+) Based on RNA Cleavage and Annealing-Accelerated Hybridization Chain Reaction, Anal. Chem. 91 (2019) 4806–4813.
[43] J. Zhao, P. Jing, S. Xue, W. Xu, Dendritic structure DNA for specific metal ion biosensor based on catalytic hairpin assembly and a sensitive synergistic amplification strategy, Biosens. Bioelectron. 87 (2017) 157–163.
[44] J. Zhuang, W. Lai, G. Chen, D. Tang, A rolling circle amplification-based DNA machine for miRNA screening coupling catalytic hairpin assembly with DNAzyme formation, Chem. Commun. (Camb) 50 (2014) 2935–2938.
[45] F. Ma, Q. Zhang, C.Y. Zhang, Catalytic Self-Assembly of Quantum-Dot-Based MicroRNA Nanosensor Directed by Toehold-Mediated Strand Displacement Cascade, Nano. Lett. 19 (2019) 6370–6376.
[46] S. Bi, S. Yue, Q. Wu, J. Ye, Triggered and catalyzed self-assembly of hyperbranched DNA structures for logic operations and homogeneous CRET biosensing of microRNA, Chem. Commun. (Camb) 52 (2016) 5455–5458.
[47] Y.S. Jiang, B. Li, J.N. Milligan, S. Bhadra, A.D. Ellington, Real-time detection of isothermal amplification reactions with thermostable catalytic hairpin assembly, J. Am. Chem. Soc. 135 (2013) 7430–7433.
[48] Z. Wu, H. Fan, N.S.R. Satyavolu, W. Wang, R. Lake, J.H. Jiang, et al., Imaging Endogenous Metal Ions in Living Cells Using a DNAzyme-Catalytic Hairpin Assembly Probe, Angew. Chem. Int. Ed. Engl. 56 (2017) 8721–8725.
[49] X. Chen, F. Hong, W. Zhang, D. Wu, T. Li, F. Hu, et al., Microchip electrophoresis based multiplexed assay for silver and mercury ions simultaneous detection in complex samples using a stirring bar modified with encoded hairpin probes for specific extraction, J. Chromatogr. A 1589 (2019) 173–181.
[50] T. Luo, L. Fan, Y. Zeng, Y. Liu, S. Chen, Q. Tan, et al., A simplified sheathless cell separation approach using combined gravitational-sedimentation-based prefocusing and dielectrophoretic separation, Lab Chip 18 (2018) 1521–1532.
[51] M. Safavieh, M.K. Kanakasabapathy, F. Tarlan, M.U. Ahmed, M. Zourob, W. Asghar, et al., Emerging Loop-Mediated Isothermal Amplification-Based Microchip and Microdevice Technologies for Nucleic Acid Detection, ACS Biomater. Sci. Eng. 2 (2016) 278–294.
[52] Y. Song, Y. Zhang, P.E. Bernard, J.M. Reuben, N.T. Ueno, R.B. Arlinghaus, et al., Multiplexed volumetric bar-chart chip for point-of-care diagnostics, Nat. Commun. 3 (2012) 1283–1292.
[53] Z. Chunsun, X. Da, Single-Molecule DNA Amplification and Analysis Using Microfluidics, Chem. Rev. 110 (2010) 4910–4947.
[54] S.K. Vashist, P.B. Luppa, L.Y. Yeo, A. Ozcan, J.H.T. Luong, Emerging Technologies for Next-Generation Point-of-Care Testing, Trends Biotechnol. 33 (2015) 692–705.
[55] L.T. Chu, H.M. Leung, P.K. Lo, T.H. Chen, Visual detection of lead ions based on nanoparticle-amplified magnetophoresis and Mie scattering, Sens. Actuators, B 306 (2020) 127564–127572.
[56] Z. Zhao, Y. Bao, L.T. Chu, J.K.L. Ho, C.C. Chieng, T.H. Chen, Microfluidic bead trap as a visual bar for quantitative detection of oligonucleotides, Lab Chip 17 (2017) 3240–3245.
[57] Z. Zhao, S. Chen, J.K. Ho, C.C. Chieng, T.H. Chen, Visual detection of nucleic acids based on Mie scattering and the magnetophoretic effect, Analyst 140 (2015) 7876–7885.
[58] R.R.B.a.G.F. Joyce, A DNA enzyme that cleaves RNA, Chem. Biol. 1 (1994) 223–229.
[59] R. Saran, J. Liu, A comparison of two classic Pb2+-dependent RNA-cleaving DNAzymes, Inorg. Chem. Front. 3 (2016) 494–501.

Minghui Wu received her B.Sc. degree in Applied Chemistry, Wuhan Polytechnic University, China in 2015 and M.Sc. in Chemical and Biochemical Engineering, Xiamen University, China in 2018. Her research interest is focused on nucleic acid based metal ion detection.

Gaobo Wang received his B.Sc. degree in Chemistry and Chemical Engineering from Henan Institute of Science and Technology, Henan, China. In 2018, he received his Master's degree in Biomedical Engineering from Korea University, Seoul, South Korea. His research interest is focused on microfluidics and nucleic acid based biosensors.

Lok Ting Chu received her B.Sc. degree in Bioengineering from City University of Hong Kong. She then joined Dr. Chen's research group in City University of Hong Kong as a full time Ph.D. candidate. Her research interest focuses on development of nucleic acid based biosensors and selective gene silencing in live cells.

Hanjin Huang is an undergraduate student at City University of Hong Kong. His research interest focuses on development of drug delivery based on precision medicine.

Ting-Hsuan Chen received his B.S. degree (2003) and M.S. degree (2005) in National Tsing Hua University, Taiwan, and obtained his Ph.D. degree in Mechanical Engineering at University of California, Los Angeles, USA (2012). He is currently an Associate Professor in Biomedical Engineering at City University of Hong Kong, Hong Kong Special Administrative Region. His research interest is leveraging the microtechnology for measurement of cell chiral mechanics and development of DNA nanosensors to detect biomarkers in live cells or visual assays for point-of-care applications